Edge states, Aharonov-Bohm oscillations, and thermodynamic and spectral properties in a two-dimensional electron gas with an antidot

E. N. Bogachek and Uzi Landman
School of Physics, Georgia Institute of Technology, Atlanta, Georgia 30332
(Received 20 March 1995; revised manuscript received 24 July 1995)

The thermodynamic and spectral properties of a two-dimensional electron gas with an antidot in a strong magnetic field, $r_c \leq r_0$, where r_c is the cyclotron radius and r_0 is the antidot effective radius, are studied via a solvable model with the antidot confinement potential $U \sim 1/r^2$. The edge states localized at the antidot boundary result in an Aharonov-Bohm-type oscillatory dependence of the magnetization as a function of the magnetic field flux through the antidot. These oscillations are superimposed on the de Haas–van Alphen oscillations. In the strong-field limit, $\hbar\omega_c \sim \epsilon_F$, where ω_c is the cyclotron frequency and ϵ_F is the Fermi energy, the amplitude of the Aharonov-Bohm-type oscillations of the magnetization due to the contribution of the lowest edge state is $\sim \mu_B k_F r_c$ (μ_B is the Bohr magneton and k_F is the Fermi wave vector). When the magnetic field is decreased, higher edge states can contribute to the magnetization, leading to the appearance of a beating pattern in the Aharonov-Bohm oscillations. The role of temperature in suppressing the oscillatory contribution due to higher edge states is analyzed. Rapid oscillations of the magnetization as a function of the Aharonov-Bohm flux, occurring on a scale of a small fraction of the flux quantum hc/e, are demonstrated. The appearance of a manifold of nonequidistant frequencies in the magneto-optical-absorption spectrum, due to transitions between electronic edge states localized near the antidot boundary, is predicted.

I. INTRODUCTION

The magnetic properties of metallic and semiconducting structures with restricted geometries are different from those in the bulk, and have been intensively studied for a long time (see, e.g., early papers by Lifshitz and Kosevich[1] and Dingle,[2] and recent reviews on size effects in orbital magnetism[3–5]). In a magnetic field the character of the motion of the electrons near the boundaries of the system changes significantly, leading, under appropriate conditions, to the formation of an interesting type of electronic state localized near the surface (the so-called edge states; see, e.g., Ref. 6). The edge states can effectively change the sample topology, transforming a simply connected geometry (e.g., solid cylinder or disk) into a doubly connected (ring) geometry. Consequently, solid-state realizations of the Aharonov-Bohm (AB) (Ref. 7) and Aharonov-Casher[8] effects become possible in simply connected samples as suggested in Ref. 9 (see also Refs. 10–15). Additionally, the current-carrying edge states play an important role in the theory of the quantum Hall effect.[16]

Progress in modern nanofabrication technology attracted recent attention to new quantum mesoscopic objects, such as dots and antidots (see, e.g., reviews in Ref. 17). In a strong magnetic field (i.e., essentially in the quantum Hall effect regime) the edge states govern the electronic properties of such systems. While these systems are seemingly similar, the physical consequences of edge states in a dot and an antidot are different. In a dot, edge states formed near the surface (outer boundary) can contribute to both thermodynamic (e.g., magnetization) and transport properties (e.g., AB oscillations[9–12]). On the other hand, in a system containing an antidot, the edge states associated with the antidot are formed inside the conductor in the vicinity of the antidot boundary. Therefore, in a large system edge states bound to an antidot (inner edge states) located far from the outer surface of the sample can contribute only to the thermodynamic properties (e.g., magnetization) of the system. Consequently, the influence of the antidot edge states (i.e., the above-mentioned inner edge states, which are sensitive to the magnetic flux through the hole constituting the antidot) on the transport properties of the system can occur only when they interact with the outer (current-carrying) edge states associated with the outer surface of the sample (see the review by Buttiker[18]). Such magnetotransport oscillations, induced by antidot edge states, have been investigated previously.[19–21]

In this paper we present a theory pertaining to the magnetization of a two-dimensional (2D) electron gas (2DEG) containing an antidot, focusing on the behavior of the system in a strong magnetic field $r_c < r_0$ (where r_c is the cyclotron radius and r_0 is the effective radius of the antidot) in the ballistic limit. The antidot is modeled by a repulsive potential[22] $U \sim 1/r^2$, which allows us to obtain an exact solution of the Schrödinger equation in the presence of applied magnetic and AB flux fields. We demonstrate that the edge states localized near the boundary of the antidot (inner hole) cause magnetization oscillations as a function of the magnetic flux through the inner hole, with a period of the order of the flux quantum hc/e. The small difference between the period of these oscillations and hc/e is due to trajectory effects in a magnetic field. These thermodynamic-type oscillations are due solely to the antidot, and in this sense they are different from simi-

0163-1829/95/52(19)/14067(11)/$06.00

lar oscillations in the magnetotransport of a conductor with a hole.[19–21] Moreover, interference between different edge states of the antidot leads, at low temperatures, to a beating pattern in the AB oscillations of the magnetization, which may be superimposed on the usual de Haas–van Alphen oscillations. Increasing the temperature suppresses the contributions from edge states with higher Landau quantum numbers. The influence of the AB flux exhibits itself in pure (hc/e) AB oscillations, whose amplitude depends on the magnitude of the magnetic field.

In addition to the influence of dots and antidots on thermodynamic and magnetotransport properties of a 2DEG in a magnetic field, they also influence its magneto-optical (MO) spectroscopic characteristics. Using the aforementioned model for an antidot in a 2DEG, we investigate the nature of MO transitions in this system, demonstrating the appearance of a rich spectrum of nonequidistant frequencies, different from the MO spectrum for a dot modeled by a harmonic confining potential.

The paper is organized as follows. In Sec. II we calculate the energy spectrum of electrons in a 2DEG with an antidot model potential in the presence of a magnetic field. Analytical and numerical analyses of the magnetization of the system are given in Sec. III, and its MO spectral properties are studied in Sec. IV. We summarize our results in Sec. V.

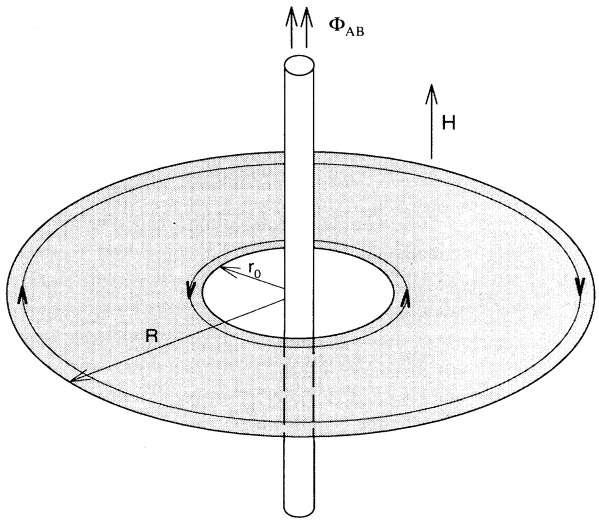

FIG. 1. Schematic description of a restricted two-dimensional electron-gas system (shaded region of radius R), with an antidot (unshaded inner region of effective radius r_0), in an applied magnetic field H, and an Aharaonov-Bohm flux, Φ_{AB}, created by an infinitely long solenoid inserted inside the antidot. Also shown are inner and outer edge states (lines with bold arrows) near the boundary of the antidot and that of the whole sample, respectively.

II. EXACTLY SOLVABLE MODEL OF A QUANTUM ANTIDOT IN MAGNETIC AND AHARONOV-BOHM FIELDS

Consider a two-dimensional electron gas with a radially symmetrical hole. We will study properties of such an antidot structure (Fig. 1) in a magnetic field and an AB field, applied simultaneously. The total Hamiltonian of the system is given by

$$H=\frac{1}{2m^*}\left[\mathbf{p}+\frac{e}{c}\mathbf{A}\right]^2+U_{AD}(\mathbf{r}) , \tag{1}$$

where m^* is an effective electron mass, $\mathbf{A}$ is the vector potential, and the model repulsive potential $U_{AD}(\mathbf{r})$ describing the antidot structure is taken as

$$U_{AD}(\mathbf{r})=\frac{B}{r^2} , \tag{2}$$

where the constant B may be related to the chemical potential ζ, and the effective radius of the antidot, r_0, by the relation

$$\zeta=\frac{B}{r_0^2} . \tag{3}$$

The vector potential $\mathbf{A}$ may be represented as a sum of two terms, $\mathbf{A}=\mathbf{A}_1+\mathbf{A}_2$ such that $\nabla\times\mathbf{A}_1=\mathbf{H}$ and $\nabla\times\mathbf{A}_2=0$, where $\mathbf{H}$ is the applied magnetic field, and $\mathbf{A}_2$ describes the additional magnetic flux Φ_{AB} created by a solenoid inserted inside the antidot (Fig. 1). Consequently, the azimuthal components of the vector potentials are given by

$$A_1^{\phi}=\frac{Hr}{2}, \quad A_2^{\phi}=\frac{\Phi_{AB}}{2\pi r} . \tag{4}$$

Substituting the wave function of the form $\psi(r,\phi)=f(r)e^{im\phi}/\sqrt{2\pi}$ into the Schrödinger equation with the Hamiltonian given in Eq. (1), we obtain the following equation for the radial function $f(r)$:

$$\frac{\partial^2 f}{\partial r^2}+\frac{1}{r}\frac{\partial f}{\partial r}+\left[\frac{2m^*E}{\hbar^2}-\frac{(m+\alpha)^2+2m^*B/\hbar^2}{r^2}-\frac{eH}{\hbar c}(m+\alpha)-\frac{e^2H^2}{4\hbar^2c^2}r^2\right]f=0 , \tag{5}$$

where $\alpha=\Phi_{AB}/\Phi_0$, and the flux quantum $\Phi_0=hc/e$. This equation yields the following expression for the energy levels of the 2DEG with an antidot, in the presence of the fields given in Eqs. (2) and (4):

$$E_{mn}=\hbar\omega_c\left[n+\frac{[(m+\alpha)^2+a^2]^{1/2}+(m+\alpha)+1}{2}\right] , \tag{6}$$

where $\omega_c=eH/m^*c$ is the cyclotron frequency, $a^2\equiv 2m^*B/\hbar^2=(k_Fr_0)^2$, k_F is the Fermi wave vector of the electron, and n and m are the radial and magnetic quantum numbers, respectively $(n=0,1,2,\ldots;$ $m=0,\pm1,\pm2,\ldots)$.

The energy levels in Eq. (6) differ from the usual Landau levels in a cylindrical coordinate system[23] [see Fig. 2(a)], to which they transform when $\alpha=0$ (i.e., $\Phi_{AB}=0$) and $a\to 0$ (i.e., when the radius of the antidot vanishes, $r_0\to 0$). While the Landau levels are degenerate for nega-

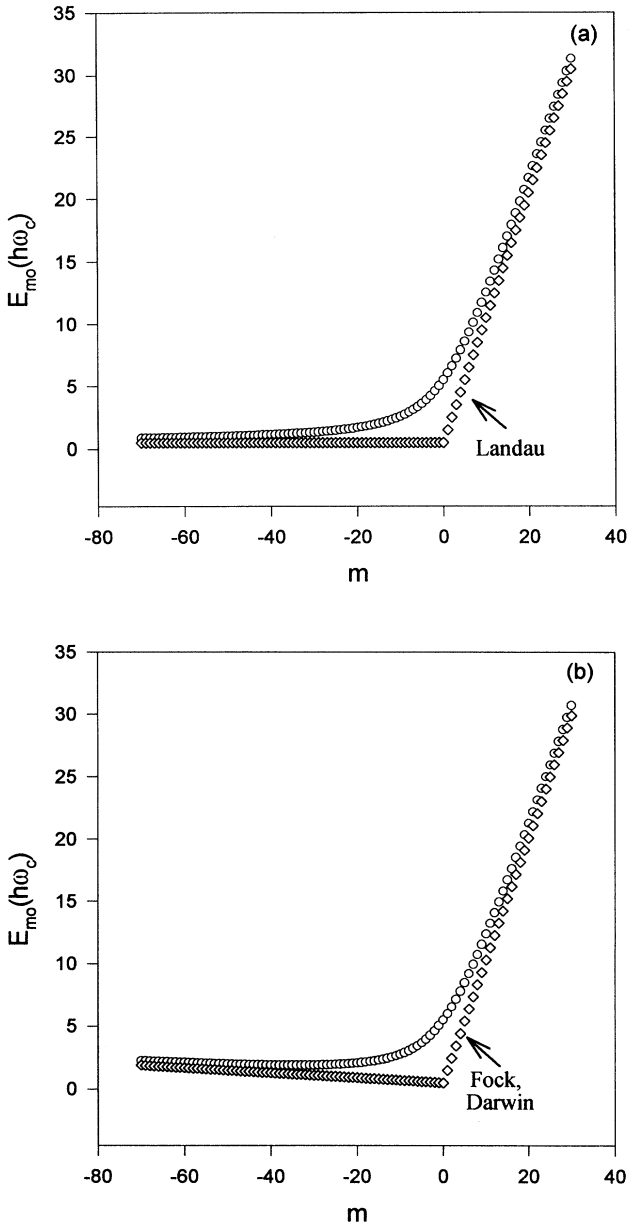

FIG. 2. The m-dependent part of the electronic energy levels E_{m0}, in units of $\hbar\omega_c$ (denoted by circles) in a two-dimensional electron gas with a hole (antidot) modeled by a potential $U_{AD}=\zeta r_0^2/r^2$ [see Eq. (2) and (3)], in an applied magnetic field, for $a=k_F r_0=10$. (a) The spectrum for an infinite system [Eq. (6)]. At the limit $a\to 0$ (that is $r_0\to 0$) the energy-level spectrum reduces to the Landau spectrum (depicted by squares). (b) The spectrum [Eq. (8)] for a restricted system with an additional parabolic confinement potential $U_D=\frac{1}{2}m\omega_0^2 r^2$ for $\omega_c/\omega=0.95$. At the limit $a\to 0$ the energy-level spectrum reduces to the Fock-Darwin spectrum. Comparison of the curves in this figure clearly demonstrates a substantial difference in their behavior for relatively small absolute values of the magnetic quantum numbers, m, corresponding to the appearance of antidot edge states in a 2DEG with a hole. On the other hand, electronic states with large negative values of m correspond to outer edge states.

tive values of m, the antidot model potential [Eq. (2)] removes this degeneracy, leading to the asymptotic degeneracy of Eq. (6) only for $m\to-\infty$. The resultant expression for the energy levels given in Eq. (6) allows us to calculate the antidot contribution to thermodynamic properties of the system. To perform such calculations it is convenient to alleviate the above-mentioned asymptotic degeneracy, corresponding to electronic states which extend to a large distance from the antidot. This can be done by including in the Hamiltonian [Eq. (1)] an additional parabolic confining potential U_D:

$$U_D(\mathbf{r})=\tfrac{1}{2}m\omega_0^2 r^2 . \tag{7}$$

This potential effectively restricts the wave functions to a finite region if we require $U_D(R)=\zeta$, where R is the effective outer radius of the sample. Consequently $\omega_0=v_F/R$, where v_F is the Fermi velocity. Using the above, the electronic levels become nondegenerate for all m and have the form

$$E_{mn}=\hbar\omega\left[n+\frac{[(m+\alpha)^2+a^2]^{1/2}+1}{2}\right]+\tfrac{1}{2}\hbar\omega_c(m+\alpha) , \tag{8}$$

where $\omega=(\omega_c^2+4\omega_0^2)^{1/2}$. For $\alpha=0$ and $a\to 0$ this formula reduces to the well-known expression for the Fock-Darwin levels[24] [see Fig. 2(b)].

In the following we limit ourself to cases with

$$R\gg r_0,\quad R\gg r_c , \tag{9}$$

where the second inequality means that $\omega_c\gg\omega_0$ in Eq. (8). Under these conditions the influence of the outer boundary of the sample on the dynamics of the electronic motion near the antidot becomes insignificant. Therefore, expression (8) for the energy levels of the electrons may be readily used for a study of the thermodynamic properties of quantum structures with an antidot in a magnetic field.

III. THERMODYNAMIC PROPERTIES

In a grand canonical ensemble (i.e., an ensemble characterized by a constant chemical potential) the thermodynamic properties are determined by the thermodynamic potential Ω:

$$\Omega=-2T\sum_{mn}\ln(1+e^{(\zeta-E_{mn})/T}) , \tag{10}$$

where T is the absolute temperature (here we express T in units of energy). Introducing the density of states and integrating twice by parts, we obtain

$$\Omega=-\frac{1}{T}\int dE\frac{g(E)e^{(E-\zeta)/T}}{(1+e^{(E-\zeta)/T})^2} , \tag{11}$$

where

$$g(E)=2\sum_{mn}(E-E_{mn})\theta(E-E_{mn}) . \tag{12}$$

Here $\theta(x)$ is the Heaviside θ function, and the multiplication by 2 is due to the electron spin.

A. Analytical analysis

We consider the magnetic response of the quantum antidot system analytically. For this purpose it is more convenient to fix the quantum number n and consider the contribution of the nth subband. Applying the Poisson summation formula to the sum over m in Eq. (12), with the energy-level spectrum given by Eq. (8), for $g(E)$ we obtain the following expression:

$$g(E)=2\hbar\omega\sum_n\sum_{k=-\infty}^{\infty}e^{2\pi ik\Phi_{AB}/\Phi_0}\times\int_{m_-^{(n)}(E)}^{m_+^{(n)}(E)}\epsilon_{mn}e^{2\pi ikm}dm\ , \tag{13a}$$

with $\epsilon_{mn}=\epsilon_n-\frac{1}{2}[(m^2+a^2)^{1/2}+bm]$, $\epsilon_n=(E/\hbar\omega)-(n+\frac{1}{2})$, $b=(\omega_c/\omega)<1$, and $m_\pm^{(n)}(E)$ are the roots of the equation $\epsilon_{mn}[m=m_\pm^{(n)}(E)]=0$, i.e.,

$$m_\pm^{(n)}(E)=\frac{-2\epsilon_n b-[4\epsilon_n^2-a^2(1-b^2)]^{1/2}}{1-b^2}\ . \tag{13b}$$

After integration by parts, for the oscillatory part of $g(E)$ we obtain

$$g^{\rm osc}(E)\simeq-\frac{\hbar\omega}{\pi^2}{\rm Re}\sum_n\sum_{k=1}^{\infty}\frac{1}{k^2}\left[\frac{\partial\epsilon_{mn}}{\partial m_+^{(n)}}e^{2\pi ikm_+^{(n)}}-\frac{\partial\epsilon_{mn}}{\partial m_-^{(n)}}e^{2\pi ikm_-^{(n)}}\right]e^{2\pi ik\Phi_{AB}/\Phi_0}\ . \tag{14}$$

Substituting Eqs. (13b) and (14) into Eq. (11), we obtain an expression for the oscillatory part of the thermodynamic potential:

$$\Omega^{\rm osc}\simeq\frac{\hbar\omega_c}{\pi^2}\sum_n\sum_{k=1}^{\infty}\frac{1}{k^2}\left\{\frac{\partial\epsilon_{mn}}{m_+^{(n)}(\zeta)}\cos\left[2\pi k\left[m_+^{(n)}(\zeta)+\frac{\Phi_{\rm AB}}{\Phi_0}\right]\right]\psi\left[\frac{2\pi^2kT}{\Delta E_+^{(n)}}\right]-\frac{\partial\epsilon_{mn}}{\partial m_-^{(n)}(\zeta)}\cos\left[2\pi k\left[m_-^{(n)}(\zeta)+\frac{\Phi_{\rm AB}}{\Phi_0}\right]\right]\psi\left[\frac{2\pi^2kT}{\Delta E_-^{(n)}}\right]\right\}, \tag{15}$$

with the function ψ and $\Delta E_\pm^{(n)}$ defined below. The functions $m_\pm^{(n)}(\zeta)$, determining the oscillatory dependence of the thermodynamic potential in the limit $R\gg r_c$, have the form

$$m_+^{(n)}(\zeta)\simeq-\frac{\Phi_{\rm in}}{\Phi_0}\frac{1}{1-\frac{\hbar\omega_c}{\zeta}(n+\frac{1}{2})}+\frac{\zeta}{\hbar\omega_c}-(n+\tfrac{1}{2})\ , \tag{16a}$$

$$m_-^{(n)}(\zeta)\simeq-\frac{\Phi_{\rm out}}{\Phi_0}+\frac{\Phi_{\rm in}}{\Phi_0}\frac{1}{1-\frac{\hbar\omega_c}{\zeta}(n+\frac{1}{2})}-\frac{\zeta}{\hbar\omega_c}+\left[\frac{\omega_c^2}{2\omega_0^2}+\frac{3}{2}\right](2n+1)\ , \tag{16b}$$

where $\Phi_{\rm in}$ is the magnetic-field flux through the antidot ($\Phi_{\rm in}=\pi r_0^2H$ and $\Phi_{\rm in}/\Phi_0=a^2/[4\zeta/\hbar\omega_c]$), and $\Phi_{\rm out}$ is the magnetic-field flux through the whole sample confined by the outer radius R ($\Phi_{\rm out}=\pi R^2H$).

The coefficients

$$\left.\frac{\partial\epsilon_{mn}}{\partial m}\right|_{m=m_\pm^{(n)}(\zeta)}=-\frac{1}{2}\left[\frac{m}{(m^2+a^2)^{1/2}}+\frac{\omega_c}{\omega}\right]\Bigg|_{m=m_\pm^{(n)}(\zeta)}$$

in Eq. (15) depend on the magnitude of the magnetic field. Taking into account the expressions

$$\frac{\Phi_{\rm out}/\Phi_0}{\epsilon_F/\hbar\omega_c}=\frac{R^2}{r_c^2},\quad\frac{\Phi_{\rm in}/\Phi_0}{\epsilon_F/\hbar\omega_c}=\frac{r_0^2}{r_c^2}\ ,\qquad\frac{a}{\epsilon_F/\hbar\omega_c}=\frac{2r_0}{r_c},\quad\frac{a}{\phi_{\rm in}/\phi_0}=\frac{2r_c}{r_0}\ , \tag{17}$$

and considering the most interesting case of strong magnetic fields

$$r_c\ll r_0 \tag{18}$$

when the edge states are confined to the proximity of the antidot, we obtain

$$\frac{\partial\epsilon_{mn}}{\partial m_-^{(n)}(\zeta)}\simeq\frac{r_c^2}{R^2}\ ,\qquad\frac{\partial\epsilon_{mn}}{\partial m_+^{(n)}(\zeta)}\simeq-\frac{r_c^2}{r_0^2}\left[1-\frac{\hbar\omega_c}{\zeta}(n+\tfrac{1}{2})\right]^2\ . \tag{19}$$

The temperature dependences of the oscillations of $\Omega^{\rm osc}$ [see Eq. (15)] are described by the standard functions $\psi(2\pi^2kT/\Delta E_\pm^{(n)})$, where $\psi(x)=x/\sinh(x)$. The corresponding values of the energies $\Delta E_\pm^{(n)}$ for magnetic fields in the range described by Eq. (18) are

$$\Delta E_{+}^{(n)} \simeq \left[\frac{2\zeta}{\hbar\omega_c} - 2n - 1 \right]^2 \frac{\hbar\omega_c}{a^2}$$
$$\simeq \left[1 - \frac{\hbar\omega_c}{\zeta}(n+\tfrac{1}{2}) \right]^2 \frac{\hbar v_F}{r_0} \frac{r_c}{r_0}$$
$$\simeq \left[1 - \frac{\hbar\omega_c}{\zeta}(n+\tfrac{1}{2}) \right]^2 \frac{\hbar^2}{m^* r_0^2} k_F r_c \ , \quad (20)$$

and

$$\Delta E_{-}^{(n)} \simeq \tfrac{1}{2}\hbar\omega \left[1 - \frac{\omega_c}{\omega} \right] \simeq \frac{\hbar v_F}{R} \frac{r_c}{R} \simeq \frac{\hbar^2}{m^* R^2} k_F r_c \ . \quad (21)$$

Differentiation of the thermodynamic potential in Eq. (15) with respect to the magnetic field gives the magnetization

$$M = -\frac{\partial \Omega}{\partial H} \ . \quad (22)$$

For the oscillatory part of M, we obtain

$$M^{\rm osc} \simeq \frac{2\hbar v_F r_c}{\Phi_0} \sum_n \sum_{k=1}^{\infty} \frac{1}{k} \left\{ \left[1 - \frac{\hbar\omega_c}{\zeta}(n+\tfrac{1}{2}) \right] \sin\left[2\pi k \left[m_{+}^{(n)}(\zeta) + \frac{\Phi_{\rm AB}}{\Phi_0} \right] \right] \psi\left[\frac{2\pi^2 kT}{\Delta E_{+}^{(n)}} \right] \right.$$
$$\left. + \sin\left[2\pi k \left[m_{-}^{(n)}(\zeta) + \frac{\Phi_{\rm AB}}{\Phi_0} \right] \right] \psi\left[\frac{2\pi^2 kT}{\Delta E_{-}^{(n)}} \right] \right\} . \quad (23)$$

The sum over n (total contribution of the n subbands) in Eqs. (15) and (23) is taken from $n=0$ to $n=n_0$, where n_0 is the index of the highest occupied n level, determined by the largest integer which satisfies the following condition [which for zero temperature is obtained by requiring that the right-hand side of Eq. (8) be smaller than $\zeta \equiv \epsilon_F$]:

$$u(n) \equiv \zeta - \hbar\omega n - E_{m0}^{\rm min} \geq 0 \ , \quad (24)$$

where $E_{m0}^{\rm min} = a\hbar\omega_0 = 2\epsilon_F r_0/R$ is the minimum value of the m-dependent part of the energy $E_{m0} = \hbar\omega/2[(m^2+a^2)^{1/2}+1] + \hbar\omega_c m/2$ [see Fig. 2(b)].

The resulting expressions, Eqs. (15) and (23), demonstrate an oscillatory behavior of the thermodynamic potential Ω and magnetization M of a two-dimensional electronic structure with a hole (antidot) in magnetic (H) and AB flux ($\Phi_{\rm AB}$) fields. We consider the case of such a strong magnetic field that $u(0) \geq 0$ and $u(1) < 0$ (i.e., when the cyclotron energy $\hbar\omega_c$ is of the order of the chemical potential). In this case only one term contributes to the sum over n, i.e., $n=0$ (this also holds for finite but low temperatures). The most interesting result is the oscillatory dependence on the magnetic flux through the antidot, $\Phi_{\rm in} = \pi r_0^2 H$, created by the magnetic field. This flux being different from the proper AB flux created by the solenoid,[7] $\Phi_{\rm AB} = \oint \mathbf{A}_2 d\mathbf{r}$, causes oscillations of the AB type whose period is close to the flux quantum, Φ_0, and is equal in our model to $\Phi_0(1 - \frac{1}{2}\hbar\omega_c/\zeta)$; note that for applied magnetic fields H in the range such that $\Phi_{\rm in}/\Phi_0 \gg 1$, variations ΔH in the applied field of the order $\Delta H \sim \Phi_0/\pi r_0^2$ yield a negligible variation of $\hbar\omega_c/\epsilon_F$. The difference between the period of the oscillations of the magnetization as a function of $\Phi_{\rm in}$ and the flux quantum Φ_0 is due to trajectory effects in a magnetic field, manifested in different magnitudes of the magnetic flux through the antidot and through the area enclosed by the electron trajectory around the antidot. In Fig. 3 we display the oscillatory dependence of the magnetization on the flux $\Phi_{\rm in}/\Phi_0$, for $\zeta/\hbar\omega_c = 1$ and $2\pi^2 T/\Delta E_{+}^{(0)} = 1$ [note that for this temperature the contribution of the term containing $\psi(2\pi kT/\Delta E_{-}^{(0)})$ in Eq. (23) is small].

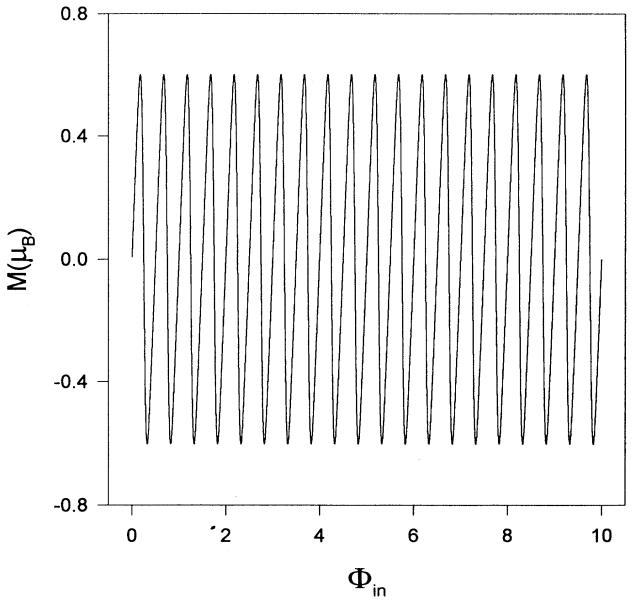

FIG. 3. Oscillatory part of the magnetization [Eq. (23)] in units of the Bohr magneton μ_B, vs the magnetic flux through the antidot, $\Phi_{\rm in} = \pi r_0^2 H$, in units of the flux quantum $\Phi_0 = hc/e$, for extremely strong magnetic fields $\zeta/\hbar\omega_c = 1$. Under this condition the only contribution to $M^{\rm osc}$ is from the $n=0$ term in Eq. (23). The data were calculated for a temperature given by $2\pi^2 T/\Delta E_{+}^{(0)} = 1$.

The reason for these oscillations is a change, caused by the magnetic flux Φ_{in}, in the number of levels $m_{\pm}^{(0)}$ lying below the Fermi energy. In the semiclassical description each oscillation corresponds to a variation of the flux through a closed electronic trajectory around the hole (antidot edge state) by one flux quantum. A decrease of the magnetic field on the scale $\Delta H \sim \zeta m^* c/\hbar e$ leads to an increase in the number n of antidot edge channels which can contribute to the magnetization [see Eq. (23)]. Increasing the temperature leads to a cancellation of the higher harmonics in the Fourier series, and to a decrease in the oscillation amplitudes.

For magnetic fields whose magnitudes are such that $u(1) \geq 0$ and $u(2) < 0$, there are contributions from two edge states with $n=0$ and 1 [i.e., two terms in the sum over n in Eq. (23)]. In this case the oscillatory behavior of the magnetization is due to the interference of two edge channels resulting in the occurrence of beats [Fig. 4(a)]. A related mechanism leading to the occurrence of beats in the magnetotransport in a wire with an antidot was discussed in Ref. 20. We also note that increasing the temperature leads to a decrease of the influence of the $n=1$ mode, and the Φ_{in} dependence of the magnetization becomes similar to the situation in stronger magnetic fields [compare Figs. 3 and 4(b)]. In the general case of magnetic fields of arbitrary strengths, the oscillatory behavior of the thermodynamic quantities becomes more complicated due to interference effects, involving many antidot edge channels, whose individual contributions occur with periods $\Delta\Phi_{in}=[1-(\hbar\omega_c/\zeta)(n+\frac{1}{2})]\Phi_0$, $n=0,1,\ldots,n_0$. It should be noted that contributions to the magnetization from higher edge channels exhibit a larger sensitivity to an increase in the temperature. The temperature dependence is described by the function $\psi(2\pi^2 kT/\Delta E_{+}^{(n)})$ in Eq. (23), with $\Delta E_{+}^{(n)}$ proportional to $[1-(\hbar\omega_c/\zeta)(n+\frac{1}{2})]^2$ [see Eq. (20)]. Consequently, increasing n causes $\Delta E_{+}^{(n)}$ to decrease, resulting in decaying contributions from such edge states.

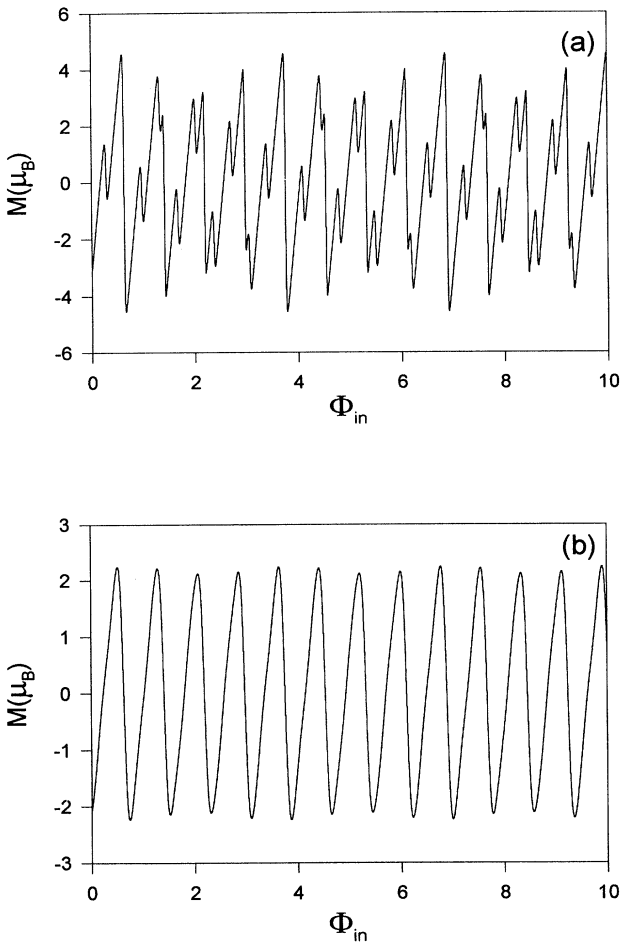

FIG. 4. Oscillatory part of the magnetization [Eq. (23)] in units of μ_B vs the magnetic flux through the antidot Φ_{in}, in units of Φ_0, for a magnetic field $\zeta/\hbar\omega_c=2.3$. In this case the two edge states, with $n=0$ and 1 contribute. (a) M^{osc} for a low temperature, $2\pi^2 T/\Delta E_{+}^{(0)}=0.1$. In this case $2\pi^2 T/\Delta E_{+}^{(1)}=0.5$ and the interference between edge states leads to a beating pattern in AB-type oscillations. (b) M^{osc} for a high temperature $2\pi^2 T/\Delta E_{+}^{(0)}=0.1$, demonstrating a suppression of the contributions from edge states with $n=1$. Compare this result with that shown in Fig. 3; note that because of the lower magnetic field in the present case the amplitude of the oscillation is larger than that shown in Fig. 3.

Another kind of oscillation of the AB type is associated with the second term in Eq. (23), containing $m_{-}^{(n)}(\zeta)$. As seen from Eqs. (23) and (16b) this term oscillates as a function of the magnetic flux through the whole sample, Φ_{out}, with a period Φ_0. This type of oscillation, due to the outer edge states, was previously investigated in weak[9,10] and strong[11,12] magnetic fields using different models. It is of importance to note that these two kinds of AB-type oscillations have different temperature dependencies because of the different lengths of the closed electronic trajectories near the inner and outer boundaries. The temperature dependence of the amplitude of the oscillations associated with the antidot edge states is determined by $T/\Delta E_{+}^{(n)}$, while that corresponding to the oscillations associated with the outer edge states (near the outer boundary of the sample) is determined by $T/\Delta E_{-}^{(n)}$. As aforementioned, in the temperature region $2\pi^2 T/E_{+}^{(0)} \sim 1$ the amplitude of the Φ_{out} oscillations, that is the second term in Eq. (23), is negligibly small (see Fig. 3).

We additionally note a third kind of oscillation described by the fourth term in Eq. (16b); that is, one proportional to $\omega_c^2/2\omega_0^2 \approx (\omega+\omega_c)/2(\omega-\omega_c)$. These oscillations are due to the magnetosize effect, and have been discussed previously.[12]

Finally, the term Φ_{AB}/Φ_0 in Eq. (23) reflects the dependence of the electronic levels [Eq. (8)] on the AB flux Φ_{AB}. Oscillations in the magnetization due to this term may be considered as a change in the Landau diamagnetism by the AB flux. It is interesting to note that unlike in the usual AB effect (see Ref. 25), the amplitude of these oscillations depends in a significant manner on the magnitude of the magnetic field (i.e., the cyclotron radius).

B. Numerical results

In this section we present results of a direct numerical calculations of the magnetization using its definition

[Eqs. (22) and (11)] and the expression in Eq. (8) for the electronic energy levels. In Fig. 5 we display the magnetic moment M (in units of μ_B, where $\mu_B = e\hbar/2m^*c$ is the Bohr magneton) as a function of the normalized cyclotron frequency $\tilde{\omega} \equiv \omega_c/\omega_0$ for $T=0$, $\zeta/\hbar\omega_0 = 100$, and $a = k_F r_0 = 20$ (in this case $R/r_0 = 10$), in the region of strong $r_c < r_0$ [Fig. 5(a)] and weak $r_c > r_0$ [Fig. 5(b)] magnetic fields. Figures 5(a) and 5(b) correspond to small and large numbers of occupied quasi-Landau-levels, respectively. In both figures we observe well defined de Haas–van Alphen oscillations which are destroyed only in the region $\omega_c/\omega_0 = R/r_c \sim 1$ in Fig. 5(b) (i.e., the region of strong magnetosize effect). In addition to the ordinary de Haas–van Alphen oscillations there is an oscillatory fine structure of AB type superimposed on the de Haas–van Alphen ones, with a significantly smaller period and amplitude (see also the curve in Fig. 6 for $T=0$). Moreover, the amplitude of the AB-type structure increases with a decrease of the magnetic field [compare Figs. 5(a) and 5(b)]. The possible coexistence of the de Haas–van Alphen and AB oscillations in a quantum dot has been discussed in Refs. 11 and 12. Unlike previous considerations, in our case the AB-type oscillatory structure is a sum of contributions from both outer (dot) and inner (antidot) edge states. These oscillations, which have different periods [the ratio of the periods $(\Delta H)_{\text{in}}/(\Delta H)_{\text{out}}$ is proportional to R^2/r_0^2], are due to the dependence of the electronic energy levels on the magnetic flux through the outer and inner boundaries.

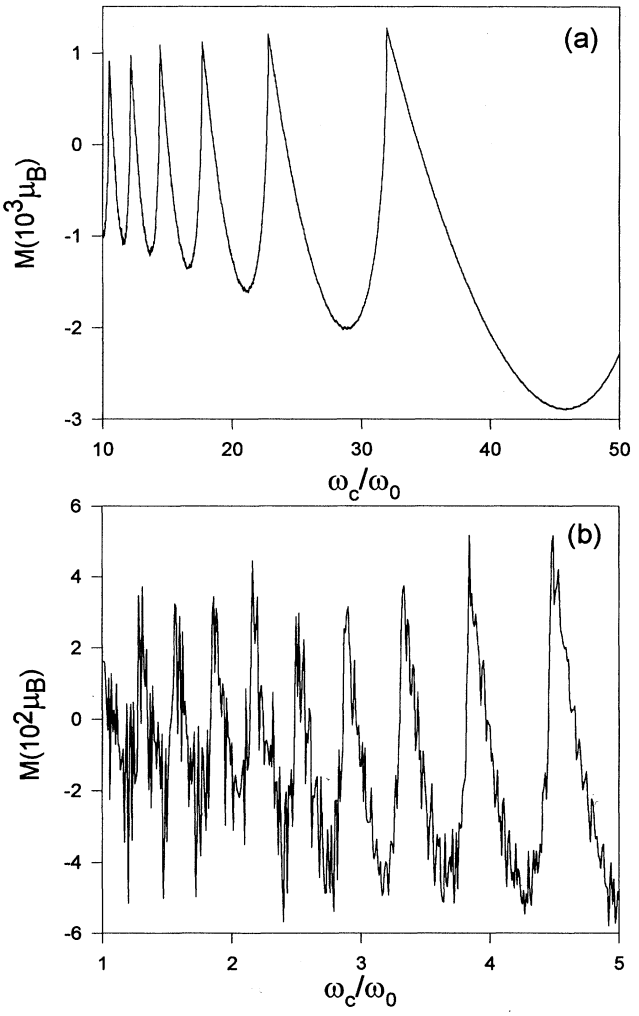

FIG. 5. The magnetization (in units of $10^3\ \mu_B$) of a 2DEG with an antidot at $T=0$, as a function of the strength of the applied magnetic field, expressed as ω_c/ω_0, where ω_c is the cyclotron frequency and $\omega_0 = v_F/R$, with R the radius of the sample. (a) and (b) correspond to strong ($r_c < r_0$) and weak ($r_c > r_0$) magnetic fields, respectively (r_0 is the effective radius of the antidot). In both cases $\epsilon_F/\hbar\omega_0 = 100$ and $a = k_F r_0 = 20$. The large oscillations in (a) correspond to the de Haas–van Alphen oscillations; note the superimposed "grass" of AB origin. For the weaker magnetic fields shown in (b), note the decrease of the amplitude of the de Haas–van Alphen oscillations, and the more pronounced AB-type oscillations.

As mentioned above, AB oscillations originating from the outer and inner edge states also have different temperature dependencies. In Fig. 6 we plot the magnetization versus the cyclotron frequency in a small interval of $\tilde{\omega}$, at different values of the temperature [the data for $T=0$ is taken from Fig. 5(a) in the interval $28 \le \tilde{\omega} \le 30$]. At $T \simeq 0.05\hbar\omega_0$ only the interference contribution originating from the inner edge states, characterized by a large period, remains. Further increase of the temperature leads to the complete disappearance of the AB oscillations (see Fig. 6 for $T = 0.2\hbar\omega_0$).

Variation of the applied magnetic field leads to a variation of the magnetic flux both through inner and outer boundaries. It is interesting to investigate the dependence of the magnetization on the magnetic flux, Φ_{in}, through the antidot, keeping the flux through the outer

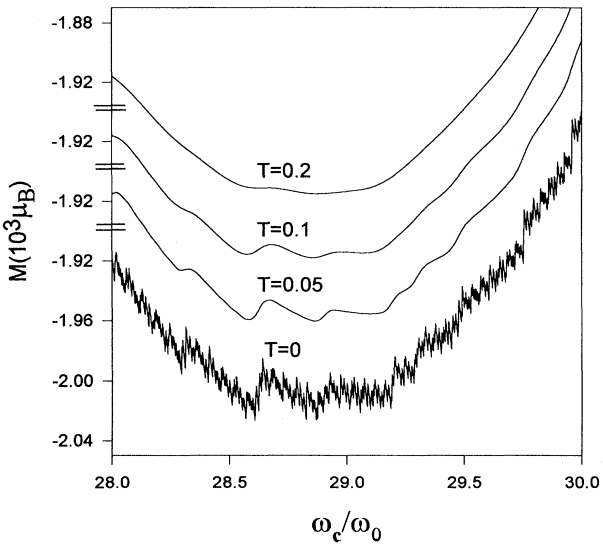

FIG. 6. Same as in Fig. 5, in the region $28 \le \omega_c/\omega_0 \le 30$ plotted for $T=0$ (taken from the corresponding data shown in Fig. 5), and for $T/\hbar\omega_0 = 0.05$, 0.1, and 0.2. Note the suppression of the oscillations due to the outer edge states at $T=0.05$, and the further suppression of the oscillations corresponding to the inner (antidot) edge states occurring at higher temperatures.

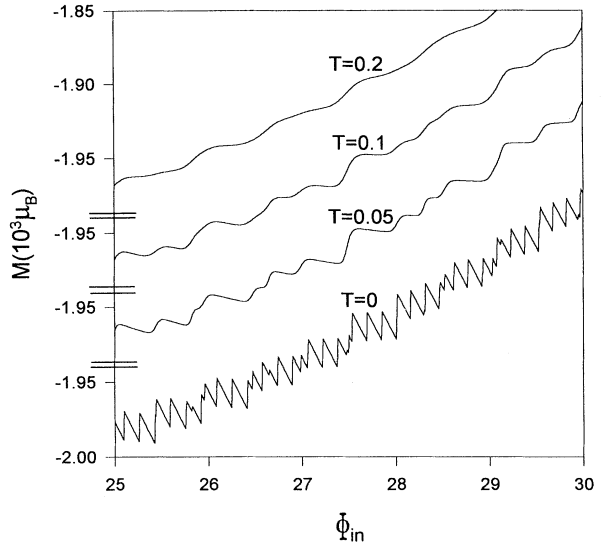

FIG. 7. The magnetization as a function of the flux through the antidot, Φ_{in} (in units of Φ_0), for $T/\hbar\omega_0=0$, 0.05, 0.1, and 0.2. These calculations were performed for $\omega_c/\omega_0=30$ and $\epsilon_F/\hbar\omega_0=100$. The oscillations are due to the inner (antidot) edge states. Note that the effect of temperature in suppressing the oscillations occurs for temperatures similar to those which suppress the oscillations due to the antidot edge states shown in Fig. 6.

boundary constant. This may be done if we vary only the inner (antidot) radius (i.e., $\Phi_{in}=\pi r_0^2 H$). Note that variation of the effective antidot radius, r_0, directly implies variation of the antidot potential, Eq. (2); such a variation may be achieved experimentally using a gate-voltage technique.[6] Figure 7 displays such a dependence (contribution of inner edge states). The characteristic period of oscillations in this case is of the same order as the period of oscillations corresponding to the inner edge states shown in Fig. 6 (compare, for instance, the curves for $T=0.05$ in Figs. 6 and 7). This further supports our conclusion that the larger period oscillations in Fig. 6 do indeed originate from the inner (antidot) edge states.

Finally, Fig. 8, portrays the pure AB effect i.e., a dependence of the magnetization on the flux Φ_{AB} created by a solenoid inserted inside the antidot. The dependence of the magnetization on the flux Φ_{AB} on a scale of a small fraction of the flux quantum should be noted, originating from a redistribution of all the energy levels caused by variation of the Φ_{AB} flux (see also Ref. 26). Additionally the amplitude of the oscillations increases for smaller applied magnetic fields [compare Figs. 8(a) and 8(b), corresponding to weak and strong magnetic fields, respectively]. Underlying this behavior is the increase of the effective region contributing to the AB effect, the size of which is proportional to the cyclotron radius.

IV. MAGNETO-OPTICAL SPECTRUM

The discrete frequency spectrum of magneto-optical transitions, due to quantization of the electronic spectrum in a magnetic field, is a well-known phenomenon.[27] In a 2DEG placed in a magnetic field the MO frequencies are proportional to the cyclotron frequency. The MO spectra in a 2DEG with dots or antidots may vary from the MO spectrum of a homogeneous 2DEG due to variations in the electronic quantization caused by the added confinement potentials creating the structures. The characteristics of MO transitions in a 2DEG dot structure have been studied recently.[17,28–30] In this section we present a theory of magneto-optical absorption in an antidot structure, modeled by a confinement potential $U\sim 1/r^2$ [see Eq. (3)]. We find that formation of edge states near the antidot boundary leads to a substantial change in the MO absorption spectrum in comparison with the usual Landau-type spectrum.

Using the model discussed in Sec. II, with $\mathbf{A}_2=0$ [see Eq. (4)], the radial function $f(r)$ in Eq. (5) (with $\alpha=0$) may be expressed in terms of the confluent hyper-

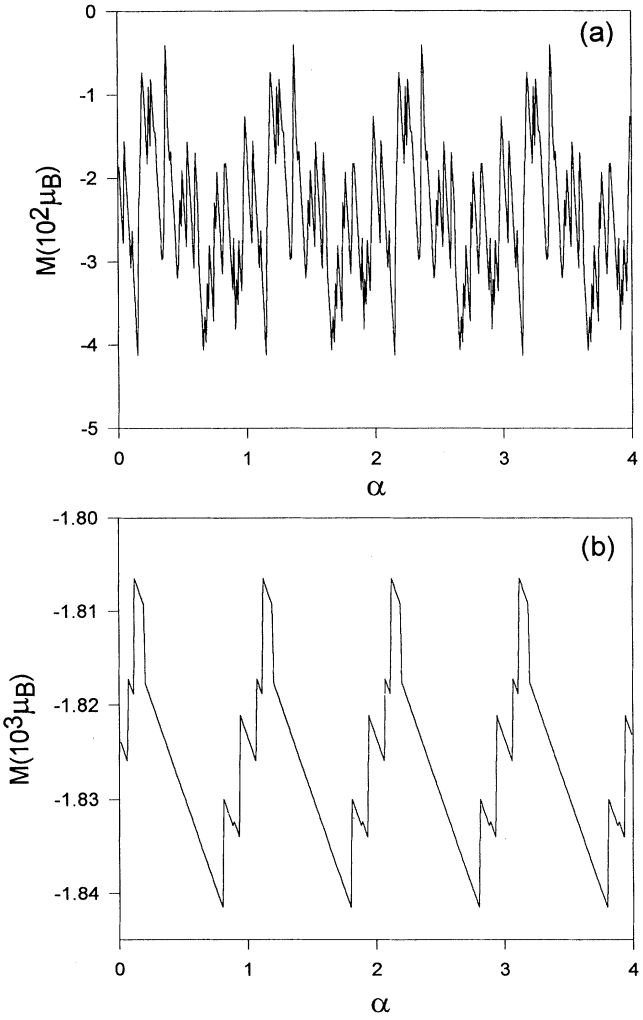

FIG. 8. The magnetization as a function of the AB flux (which may be created by inserting a solenoid inside the dot; see Fig. 1), expressed as $\alpha=\Phi_{AB}/\Phi_0$. The results in (a) were calculated for a weak magnetic field, $\omega_c/\omega_0=3$ and $\Phi_{in}/\Phi_0=3$. The results shown in (b) were calculated for a strong magnetic field $\omega_c/\omega_0=30$ and $\Phi_{in}/\Phi_0=30$. In both cases $\epsilon_F/\hbar\omega_0=100$.

geometric function ${}_1F_1(a,b,c)$. Taking into account the boundary condition for the wave function (i.e., a finite value at $r\rightarrow\infty$) we obtain

$$f(r)=C_{mn}^{-1/2}e^{-r^2/4l_H^2}\left[\frac{r^2}{2l_H^2}\right]^{A_m/2}\times{}_1F_1\left[-n,A_m+1,\frac{r^2}{2l_H^2}\right]. \quad (25)$$

Here $l_H=(\hbar c/eH)^{1/2}$ is the magnetic length, $A_m=(m^2+2m^*B/\hbar^2)^{1/2}=(m^2+k_F^2r_0^2)^{1/2}$, k_F is the Fermi wave vector, and n is a non-negative integer. The normalization constant C_{mn} is determined by the integral

$$C_{mn}=l_H^2\int_0^\infty dx\, e^{-x}x^{A_m}[{}_1F_1(-n,A_m+1,x)]^2 . \quad (26)$$

The eigenenergies corresponding to the eigenfunctions are given by Eq. (6) (with $\alpha=0$), where as noted before in the limit $r_0\rightarrow 0$ the energy levels reduce to the usual Landau levels in a cylindrical coordinate system [see Fig. 2(a)]. Additionally, comparison of the curves in Fig. 2(a) clearly demonstrates a substantial difference in their behavior for relatively small absolute values of the magnetic quantum numbers m, corresponding to the appearance of the antidot edge states in a 2DEG with a hole. Therefore, the single-electron wave functions and the energy-level spectrum of a 2DEG with an antidot potential describe all the electronic states in the system, including edge states formed near the antidot boundary.

The MO absorption in such a system is determined by the probability of transitions between the states $\psi_{mn}(\mathbf{r})$ and $\psi_{m'n'}(\mathbf{r})$, which is proportional to the square of the interaction energy.[27] For the interaction between the oscillating electric field and the electric dipole moments of the electrons (we restrict ourselves to the dipole approximation) the transition amplitude $A_{mn}^{m'n'}$ and associated oscillator strength $f_{mn}^{m'n'}$ are given by

$$A_{mn}^{m'n'}=\langle\psi_{mn}|re^{\pm i\phi}|\psi_{m'n'}\rangle , \quad (27)$$

$$f_{mn}^{m'n'}=\frac{2m^*}{\hbar}\omega_{mn}^{m'n'}|A_{mn}^{m'n'}|^2 , \quad (28)$$

where $\omega_{mn}^{m'n'}=(E_{m'n'}-E_{mn})/\hbar$ is the transition frequency.

Integration over the angle Φ results in the selection rule $\Delta m\equiv m'-m=\pm 1$ for the allowed transitions, and the expression for the amplitude $A_{mn}^{m'n'}$ is given by

$$A_{mn}^{m'n'}=\delta_{m,m'\pm1}\sqrt{2}l_H^3C_{mn}^{-1/2}C_{m'n'}^{-1/2}\times\int_0^\infty dX\, e^{-X}X^{1/2(A_m+A_{m'}+1)}\times{}_1F_1(-n,A_m+1,X)\times{}_1F_1(-n',A_{m'}+1,X) . \quad (29)$$

Analysis of the integral in Eq. (29) shows that transitions are allowed with an arbitrary change of the quantum number n (there is no rigorous selection rule for n). In this sense the magneto-optical behavior in the antidot system is similar to the situation for a dot described by a hard wall confining potential.[29] In this context we note that for a dot with a harmonic confining potential the allowed MO transitions are governed by rigorous selection rules for both n and m quantum numbers.[28,29]

The absence of rigorous selection rules for the n transitions leads to the following expression for the allowed frequencies of the MO transitions caused by the antidot:

$$\omega_{mn}^{m'n'}=\omega_c\Delta n+\tfrac{1}{2}\omega_c g_\pm(m) , \quad (30a)$$

$$g_\pm(m)=\sqrt{(m\pm1)^2+(k_Fr_0)^2}-\sqrt{m^2+(k_Fr_0)^2}\pm1 . \quad (30b)$$

For $\Delta n=0$, only $g_+(m)$ should be used. The function $g_+(m)$, which describes the m-dependent part of the transitions frequencies, is plotted in Fig. 9.

The main characteristic of the magneto-optical transitions in the presence of an antidot is the appearance of a rich spectrum with many frequencies (as opposed to only two frequencies in the case of a dot modeled by a harmonic confining potential[28,29]), due to the nonequidistant electronic energy levels [Eq. (6) with $\alpha=0$] and the absence of a selection rule for transitions involving changes of the n quantum number. For each value of Δn there is a manifold of transition frequencies corresponding to the different quantum numbers m (see Fig. 10). The transition frequencies between electronic edge states near the antidot depend on the size of the antidot and the magnetic quantum number m which determine the spacings between the energy levels. A linear dependence of the transition frequencies on the magnetic field, with a slope proportional to $g(m)$, should also be noted (Fig. 10). Moreover, when the magnetic field tends to zero, the transition frequency in antidot structure vanishes, unlike the corresponding behavior in a dot structure where the finite value of the transition frequency at a zero field is due to the quantum-size effect. The magneto-optical transition frequencies $\omega_{mn}^{m+1,n'}$ corresponding to transitions between antidot edge states [i.e., the region of small absolute

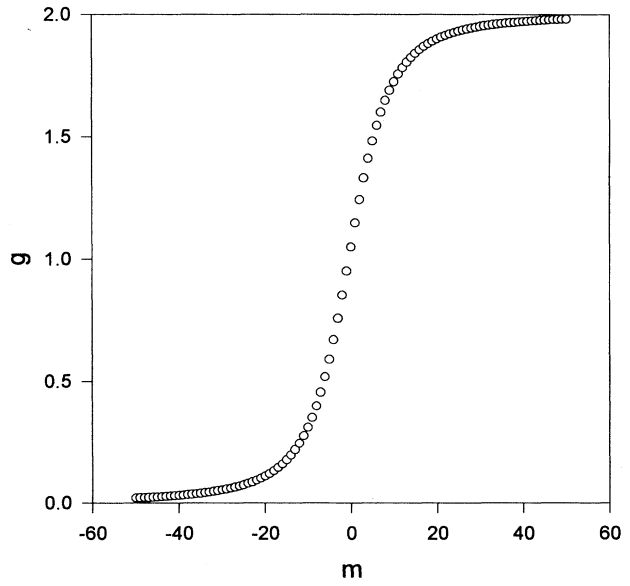

FIG. 9. The function $g_+(m)$ describing the m-dependent part of the transition frequencies [Eq. (30)] for $k_Fr_0=10$.

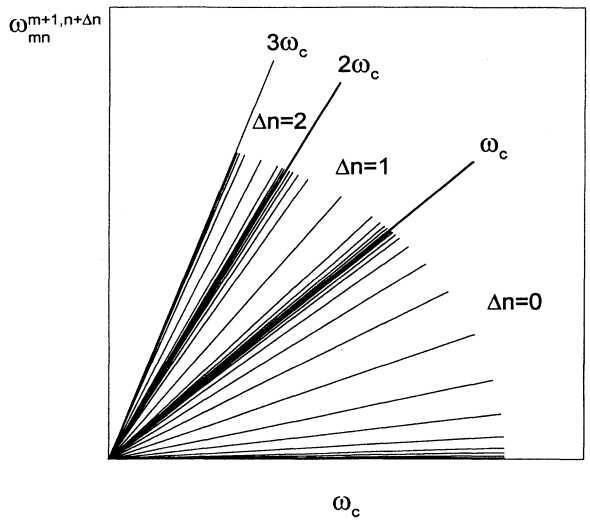

FIG. 10. Schematic of the MO transition frequencies, $\omega_{mn}^{m+1,n+\Delta n}$, in a 2DEG with an antidot plotted vs the cyclotron frequency ω_c for transitions between different edge states characterized by the quantum numbers m. The fundamental frequencies, which are given by integer multiples of the cyclotron frequency corresponding to transitions between bulk Landau levels, are denoted by longer lines marked ω_c, $2\omega_c$, $3\omega_c$, etc.

values of the quantum numbers m; see Figs. 2(a) and 9] have a discrete character and differ from the fundamental frequencies which are proportional to the cyclotron frequency and correspond to transitions between bulk Landau levels.[27] Finally, for electronic states with larger absolute values of m [i.e., $|m| \gg k_F r_0$; these values correspond to electronic states localized far from the antidot; Fig. 2(a)] the spectrum of the transition frequencies becomes quasicontinuous and converges to the fundamental frequencies.

V. CONCLUSIONS

In this paper we have studied the magnetic and magneto-optical properties of a 2DEG with a hole (antidot) in the strong magnetic-field regime. Using a simple model for the antidot potential allowed us to obtain analytical solutions, unlike the often used tight-binding model treatment[11,19] which can only be solved numerically.

Edge states formed near the antidot (inner boundary) manifest themselves in AB-type oscillations of the magnetization. In the ultraquantum limit ($\hbar\omega_c \sim \zeta, r_c \ll r_0$) the amplitude of the magnetization oscillations M_0 is, according to Eq. (23),

$$M_0 \sim \mu_B k_F r_c \ , \tag{31}$$

It is suggested that the magnetic moment in such a system could be measured (for reports of measurements of the magnetic moments of single metallic and semiconducting rings of mesoscopic size, see Refs. 31 and 32). These oscillations exist for temperatures $T \lesssim (\hbar^2/m^* r_0^2) k_F r_c$. Decreasing the magnetic field leads to the onset of additional edge states with higher n quantum numbers, and to the appearance of beats in the magnetization as a function of the field. It is interesting that contributions of higher edge states to the magnetization may be suppressed by temperature [see Eqs. (20) and (23) and Fig. 4].

The oscillations of the magnetization induced by the antidot edge states are of thermodynamic nature, can exist in a ballistic limit, and differ from those in magnetotransport where backscattering of edge states is necessary.[18]

Although here we have treated only the ballistic limit, it is well known that in the quantum Hall effect regime a single impurity cannot backscatter edge-state electrons.[33] Consequently, we expect that the thermodynamic oscillations induced by the edge states which we have discussed will occur for systems and conditions where the electron mean free path path l is larger than the cyclotron radius, i.e., when $l \gg r_c$.

It should be noted in conclusion that the amplitude of such thermodynamic oscillations may be increased if we consider antidot arrays under the conditions $r_c < d$ (where d is the distance between antidots) and $r_0 \ll l$. The latter condition is necessary in order to exclude effects due to scattering by impurities which can randomize the phases of the wave functions of electrons populating the edge states localized near the antidots.

Using the same model for an antidot in a 2DEG, we have investigated the magneto-optical spectroscopic characteristics of the system. The nature of the electronic energy levels in this system, and the absence of a rigorous selection rule for transitions involving changes of the n quantum number, underlie the appearance of a rich spectrum with many frequencies (Fig. 10). The dependence of the transition frequencies between electronic edge states near the antidot on the size of the antidot could be used for spectroscopic characterization of such systems.

ACKNOWLEDGMENTS

This research is supported by the U.S. DOE (Grant No. DE-FG05-86ER-45234) and the AFOSR. Computations were performed at the Georgia Institute of Technology Center for Computational Materials Science.

[1] I. M. Lifshitz and A. M. Kosevich, Dokl. Akad. Nauk USSR **91**, 795 (1953); A. M. Kosevich and I. M. Lifshitz, Zh. Eksp. Teor. Fiz. **29**, 743 (1955) [Sov. Phys. JETP **2**, 646 (1956)].

[2] R. B. Dingle, Proc. R. Soc. London Ser. A **212**, 47 (1952); **216**, 118 (1953); **219**, 463 (1953).

[3] B. Shapiro, Physica A **200**, 498 (1993).

[4] J. M. van Ruitenbeek and D. A. van Leeuwen, Mod. Phys. Lett. B **7**, 1053 (1993).

[5] D. Yoshioka and H. Fukuyama, J. Phys. Soc. Jpn. **61**, 2368 (1992).

[6]C. W. J. Beenakker and H. van Houten, in *Solid State Physics,* edited by H. Ehrenreich and D. Turnbull (Academic, San Diego, 1991), Vol. 44, p. 1.
[7]Y. Aharonov and D. Bohm, Phys. Rev. **115**, 485 (1959).
[8]Y. Aharonov and A. Casher, Phys. Rev. Lett. **53**, 319 (1984).
[9]E. N. Bogachek and G. A. Gogadze, Zh. Eksp. Teor. Fiz. **63**, 1839 (1972) [Sov. Phys. JETP **36**, 973 (1973)]; E. N. Bogachek, Fiz. Nizk. Temp. **2**, 473 (1976) [Sov. J. Low Temp. Phys. **2**, 235 (1976)].
[10]N. B. Brandt, D. V. Gitsu, A. A. Nikolayeva, and Ya. G. Ponomarev, Pis'ma Zh. Eksp. Teor. Fiz. **24**, 304 (1976) [JETP Lett. **24**, 272 (1976)]; Zh. Eksp. Teor. Fiz. **72**, 2332 (1977) [Sov. Phys. JETP **45**, 1226 (1977)]; N. B. Brandt, E. N. Bogachek, D. V. Gitsu, G. A. Gogadze, I. O. Kulik, A. A. Nikolayeva, and Ya. G. Ponomarev, Fiz. Nizk. Temp. **8**, 718 (1982) [Sov. J. Low. Temp. Phys. **8**, 358 (1982)].
[11]U. Sivan and Y. Imry, Phys. Rev. Lett. **61**, 1991 (1988); U. Sivan, Y. Imry, and C. Hartzstein, Phys. Rev. B **39**, 1242 (1989).
[12]Y. Meir, O. Entin-Wohlman, and Y. Gefen, Phys. Rev. B **42**, 8351 (1990).
[13]P. H. M. van Loosdrecht, C. W. J. Beenakker, H. van Houten, J. G. Williamson, B. J. van Wees, J. E. Mooij, C. T. Foxon, and J. J. Harris, Phys. Rev. B **38**, 10 162 (1988).
[14]L. I. Glazman and M. Jonson, Phys. Rev. B **41**, 10 686 (1990).
[15]E. N. Bogachek and U. Landman, Phys. Rev. B **50**, 2678 (1994).
[16]B. I. Halperin, Phys. Rev. B **25**, 2185 (1982).
[17]T. Chakraborty, Comments Condens. Mater. Phys. **16**, 35 (1992); T. Chakraborty and P. Pietilainen, in *Transport Phenomena in Mesoscopic Systems,* edited by H. Fukuyama and T. Ando, Springer Series in Solid State Sciences Vol. 109 (Springer-Verlag, Berlin, 1992), p. 61; D. Heitmann and J. P. Kotthaus, Phys. Today **48** (6), 56 (1993).
[18]M. Buittiker, Semicond. Semimetals **35**, 191 (1992).
[19]Y. Takagaki and D. K. Ferry, Phys. Rev. B **48**, 8152 (1993).
[20]G. Kirczenow, A. S. Sachrajda, Y. Feng, R. P. Taylor, L. Henning, J. Wang, P. Zawadzki, and P. T. Coleridge, Phys. Rev. Lett. **72**, 2069 (1994); G. Kirczenow, Phys. Rev. B **50**, 1649 (1994).
[21]P. J. Simpson, C. J. B. Ford, D. R. Mace, I. Zailer, M. Yosefin, M. Pepper, J. T. Nicholls, D. A. Ritchie, J. E. F. Frost, M. P. Grimshaw, and G. A. C. Jones, Surf. Sci. **305**, 453 (1994).
[22]The same potential was used for an analysis of the magnetic susceptibility of a single crystal with a cylindrical cavity in the paper by E. N. Bogachek and I. O. Kulik, Fiz. Nizk. Temp. **9**, 398 (1983) [Sov. J. Low Temp. Phys. **9**, 202 (1983)].
[23]L. D. Landau and E. M. Lifshitz, *Quantum Mechanics* (Pergamon, Oxford, 1977).
[24]V. Fock, Z. Phys. **47**, 446 (1928); C. G. Darwin, Proc. Cambridge Philos. Soc. **27**, 86 (1930).
[25]I. O. Kulik, Pis'ma, Zh. Eksp. Teor. Fiz. **11**, 407 (1970) [JETP Lett. **11**, 275 (1970)].
[26]E. N. Bogachek, M. Jonson, R. I. Shekhter, and T. Swahn, Phys. Rev. B **47**, 16 635 (1993); **50**, 18 341 (1994).
[27]R. B. Dingle, Proc. R. Soc. London Ser. A **212**, 38 (1952).
[28]C. T. Liu, K. Nakamura, D. C. Tcui, K. Ismail, D. A. Antomiadis, and H. I. Smith, Appl. Phys. Lett. **55**, 168 (1989).
[29]F. Geerinckx, F. M. Peeters, and J. T. Devreese, J. Appl. Phys. **68**, 3435 (1990).
[30]T. Chakraborty, V. Halonen, and P. Pietilainen, Phys. Rev. B **43**, 14 289 (1991).
[31]V. Chandrasekhar, R. A. Webb, M. J. Brady, M. B. Ketchen, W. J. Gallagher, and A. Kleinsasser, Phys. Rev. Lett. **67**, 3578 (1991).
[32]D. Mailly, C. Chapelier, and A. Benoit, Phys. Rev. Lett. **70**, 2020 (1993).
[33]M. Büttiker, Phys. Rev. B **38**, 9375 (1988).

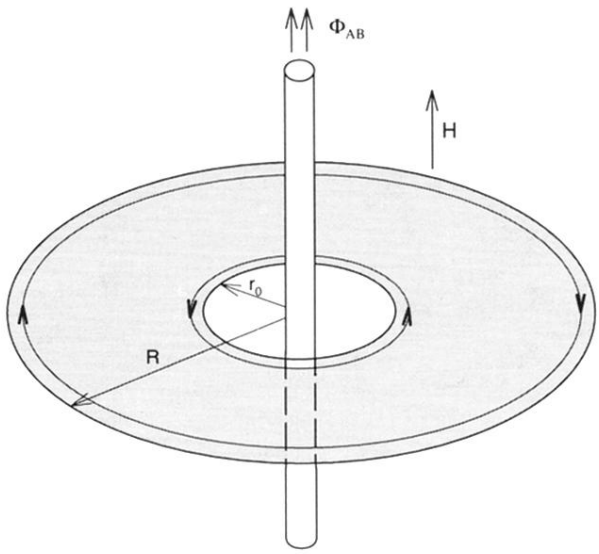

FIG. 1. Schematic description of a restricted two-dimensional electron-gas system (shaded region of radius R), with an antidot (unshaded inner region of effective radius r_0), in an applied magnetic field H, and an Aharaonov-Bohm flux, Φ_{AB}, created by an infinitely long solenoid inserted inside the antidot. Also shown are inner and outer edge states (lines with bold arrows) near the boundary of the antidot and that of the whole sample, respectively.